Physical Processes underlying the Equatorial (Geomagnetic) Effects of Solar Wind Dynamic Pressure (P_d) Variations

J. H. Sastri

Solar-Terrestrial Physics

Indian Institute of Astrophysics

Bangalore 560 034, India

E-mail:jhs@iiap.res.in

11/28/2006- UN/NASA workshop on IHY& Basic Space Science

Ecliptic Solar Wind (SW) Plasma and Interplanetary Magnetic Field (IMF) at 1 AU

- SW Parameters: N (/cc), V (km/s), ion composition,

  dynamic pressure, P_d (nPa)

- IMF Parameters: B (nT), B_x / B_y /B_z

- none of the above parameters *seldom steady* -- high temporal variability;

  'notorious' IMF Bz that regulates energy transfer from the solar wind to the magnetosphere, e.g., Akasofu's coupling function

- TWO types of P_d variation at sub-solar magnetopause:

(1) step-like increases in P_d due to fast forward IP shocks (link events on the SUN to the Terrestrial disturbances)

Terrestrial effects ↙ ↘ solar aspects

(driver-shock associations)

↓ ↓ ↓

* sudden magnetospheric compression

↓ ↓ ↓

storm sudden commencement (ssc) /sudden positive impulse (si^+) AND

followed, at times, by a substorm (controversial!) and pulsations

** sudden decreases in Pd (tangential discontinuity) ⇨ sudden magnetospheric expansion

↓ ↓ ↓

sudden negative impulse (si^-) - not as well-studied as ssc

(2) slower enhancements in Pd (both quiet and disturbed times)- relatively new and emerging dimension

Studies of *ssc*- historical perspective

- Adams (1892), Ellis (1892)- original reports of almost simultaneous global occurrence of *ssc*- IPY1
- Chapman & Ferraro (1931/32/33)- pioneering theory of interaction between solar corpuscular stream with geomagnetic field- inference of a magnetosphere – IPY2
- Gold (1955)- noting *ssc* follow solar flares, postulated the presence of shock at the leading edge of plasma cloud ejected from a flare - sharp rise of *ssc*
- IGY (1957-58)- deployment of rapid-run magnetographs- boost to ground based studies of *ssc*
- 1960's – Parker- theoretical prediction of solar wind ; and confirmation from in-situ data Neugebauer and Snyder (1962); observations of IP shocks (Sonnet et al, 1964)
- 1964- seminal work of Tamao- MHD wave propagation of compressional waves induced by IP shocks
- realization- ground-level *ssc* waveform - strong function of lat. and local time- NOT JUST A COMPRRESION EFFCT
- 1977- physical model of ssc disturbance- decomposition into those of polar origin (DP) and DL – electrical coupling of high latitude-low latitude ionospheres
- 1980's-till now - 3-D structure of ssc, improvement of time-resolution and sensitivity of GB magnetometers, establishments of networks (CPMN, 210MM, CANOPUS, IMAGE, MACSS, IGPP/LANL, Indian network, SAMBA)
- controversy regarding origin of low latitude PI- Chi et al (2001) interpretation in terms of MHD waves as originally proposed by Tamao- questioning of the earth-ionosphere wave guide model of Kikuchi and Araki (1979)
- Chi et al (2005)- consolidation of interpretation with numerical MHD simulation of PI
  - travel-time magnetoseismology- remote sensing of magnetospheric plasma using ssc/si events

¤ 2006- several fundamental questions remain unsettled regarding (equatorial) *ssc*

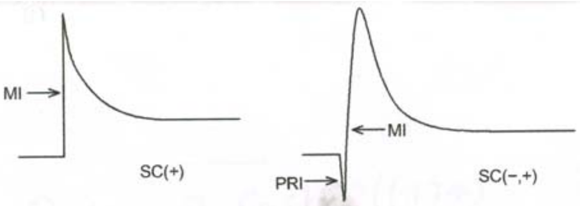

Two basic forms of *ssc* at dayside dip equator: *ssc*(+) *and ssc** (-,+)

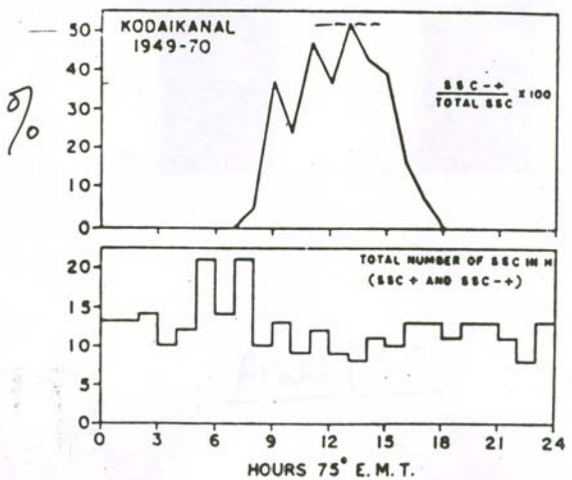

Rastogi and Sastri, 1974

	Occurrence probability (%)	Type of SSC: Dayside equator	Afternoon side: Middle lat.	Afternoon side: High lat.	Onset time
1	30–40	SC	SC	SC	Almost simultaneous at all stations
2	60–70	SC*	SC	SC*	Late in middle latitude stations where the SSC is recorded as SC
3	rare	SC*	SC*	SC*	Almost simultaneous at all stations

Global picture

Araki, 1977

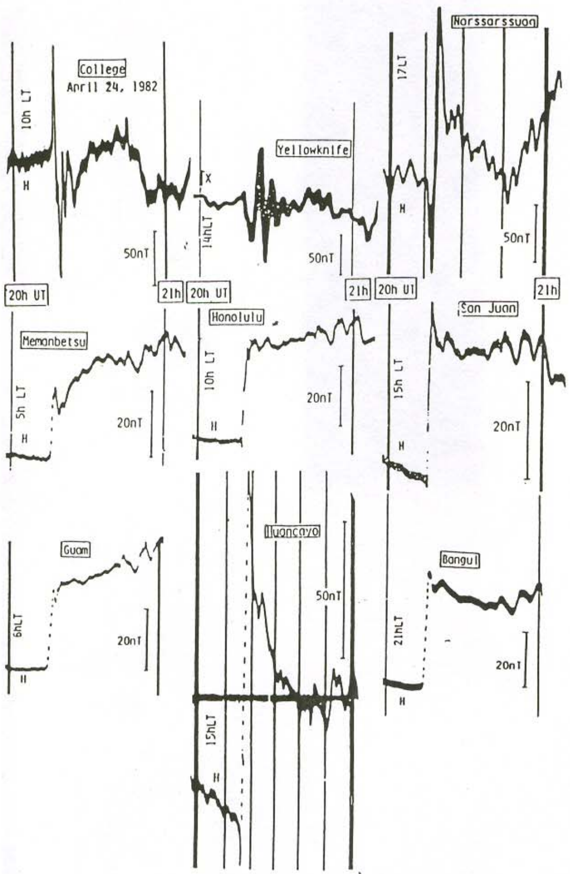

Simultaneous observations of an SC at auroral (upper panels), middle and low latitudes (middle panels), as well as the equator (lower panels). Left and right panels correspond to morning and afternoon, respectively.

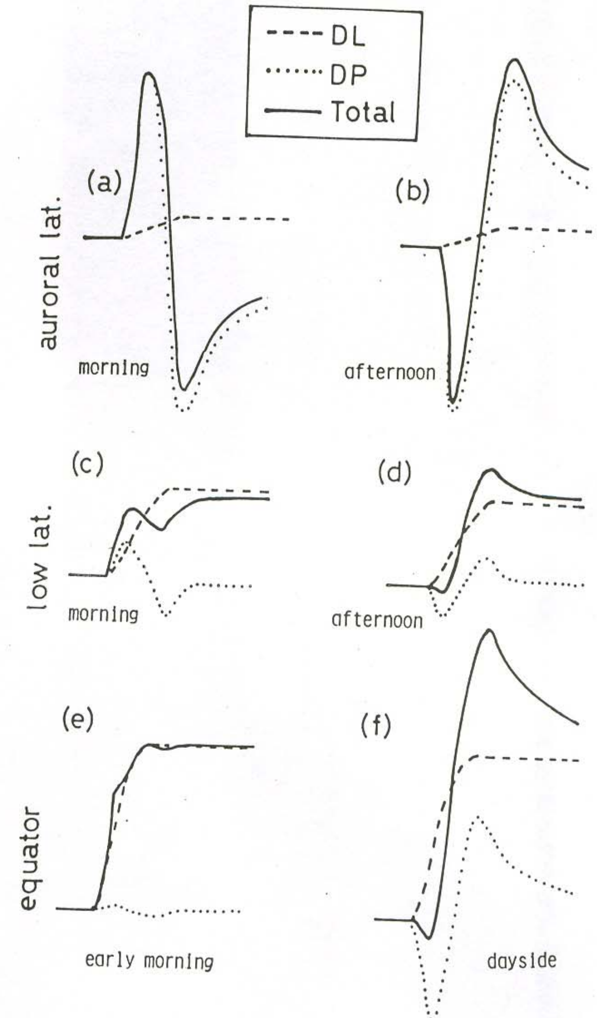

Decomposition of the SC disturbance field into *DP*- and *DL*-sub-fields.

Araki, 1977

D_{sc}= DL + DP

DP-disturbance of polar origin &

DL-disturbance that predominates at low latitudes-basically compression effect

DP= DP_{pi} + DP_{mi}

2-pulse structure not detected in IP space & at geosynchronous orbit

KIKUCHI ET AL.:

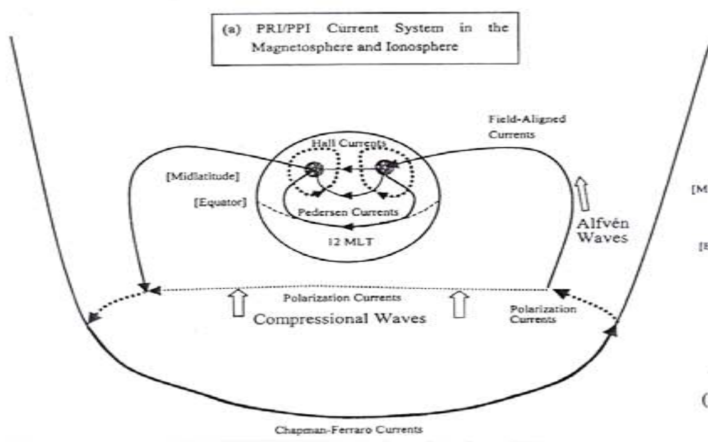

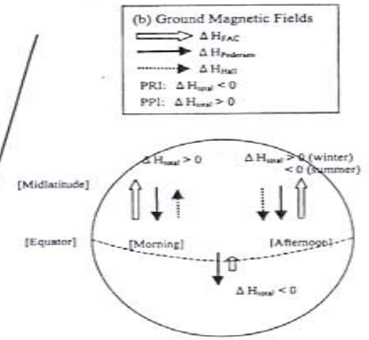

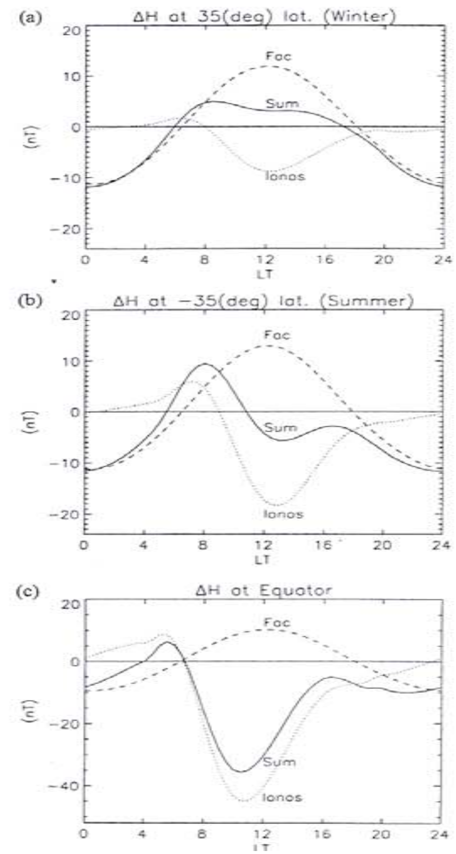

Kikuchi et al., Vol 106, 15,555, 2001

Earth-ionosphere wave guide model for *pri* of equatorial *ssc**

Kikuchi & Araki, 1979

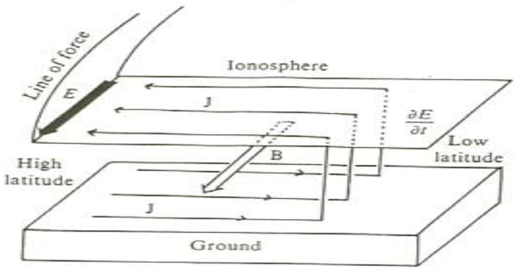

Fig. 13. Transmission of an ionospheric horizontal electric field from high latitudes to the equator [Kikuchi and Araki, 1979b].

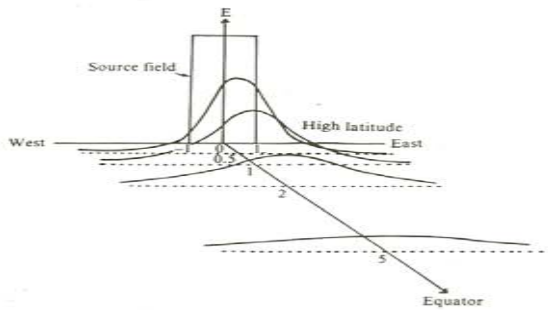

Fig. 2 Attenuation of electric fields due to finite scale of a source field. Distance in the north–south direction is normalised by the east–west scale of the source field.

well supported by HF Doppler observations of ionospheric vertical plasma motion- E-fields

Simultaneous occurrence of pri at dayside dip equator and at afternoon high latitudes

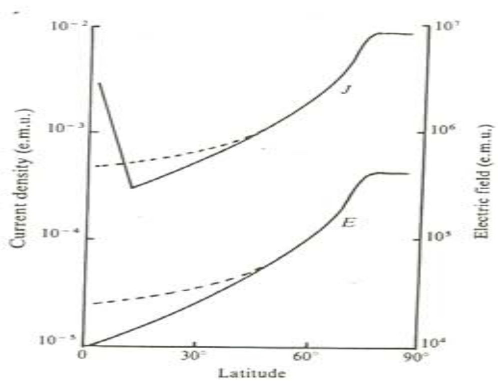

Fig. 3 Latitudinal variation of electric fields, **E**, and currents, **J**, at noon (1200 h, solid line) and midnight (0000 h, dashed line). The ionospheric conductivity is assumed to be isotropic and uniform at all latitudes on the night-time and at latitudes greater than 10° on the day-time. In the day-time equatorial region, it varies sinusoidally with local time and is maximum (10.5 times the uniform value) at the noon equator.

Observational Evidence for non-simultaneous occurrence of *pri*

Chi et al, 2001

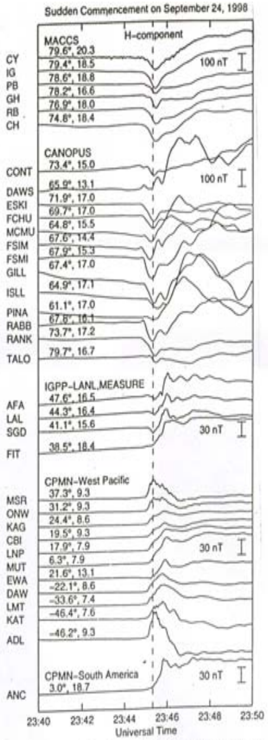

Figure 2. Time series of magnetic field in the *H* component recorded by the thirty-five stations studied in this study. The two numbers on the top of each trace are the magnetic latitude and magnetic local time of the station when the SC occurred. The dashed vertical line is plotted at 2345:20 UT as a reference time.

Original data

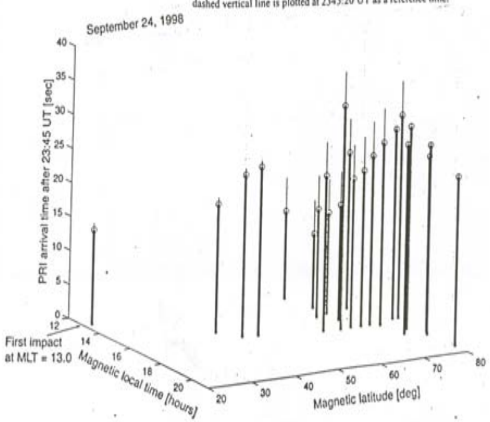

Latitudinal dependence of travel time

Alternative interpretation of *pri* of *ssc** in terms of MHD wave propagation

Chi et al, JGR-A, 106, 18,857, 2001

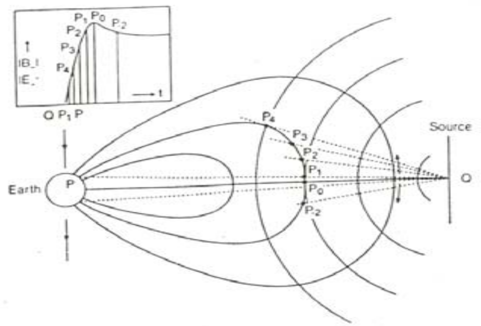

Figure 4. Schematic illustration of the propagation of MHD waves from a point source Q to a ground observer *P*. In addition to the compressional (fast) mode wave directly from the source, the observer *P* also sees Alfven waves converted from the fast mode everywhere along the field line such as P_{-2}, P_0, P_1, etc. The inset shows the temporal variation of B_H at P [After *Tamao*, 1964b].

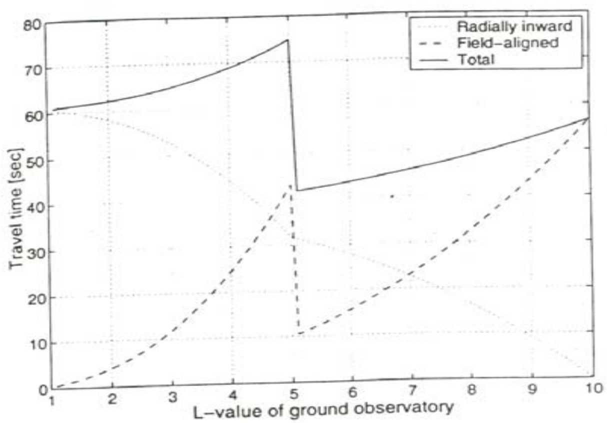

Figure 5. Travel time of MHD waves from a point source at *L*=10 at the equator to ground observatories at different *L* values. The total travel time consists of the time from the source to the field line on the equator (dotted line) and the time from the equator to the ground along the magnetic field (dashed line).

Chi et al., JGR-A, Vol 111, A08205, 2006

Numerical MHD simulation

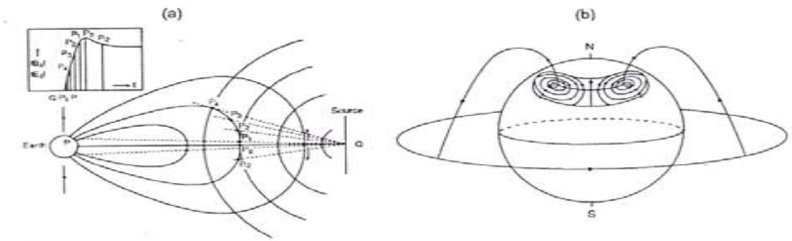

Figure 1. Two major features of Tamao's model of preliminary impulses: (a) travel paths of an impulse via MHD waves and the expected response in ground records and (b) twin vortices in the ionosphere as a result of impulse propagation.

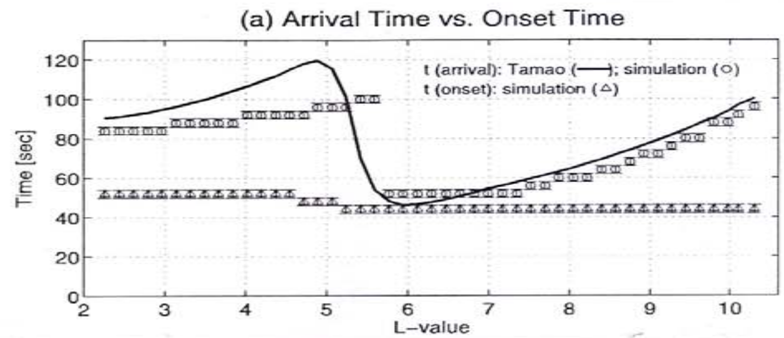

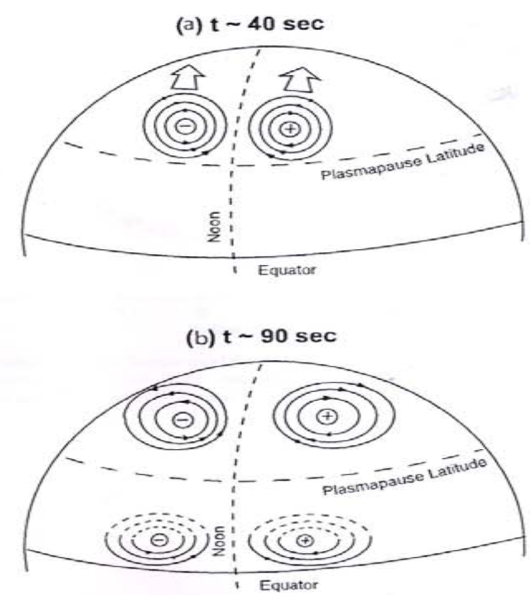

Figure 8. PI-induced twin vortices of ionospheric currents and their dynamics: (a) earlier and (b) later stages.

SASTRI ET AL.:

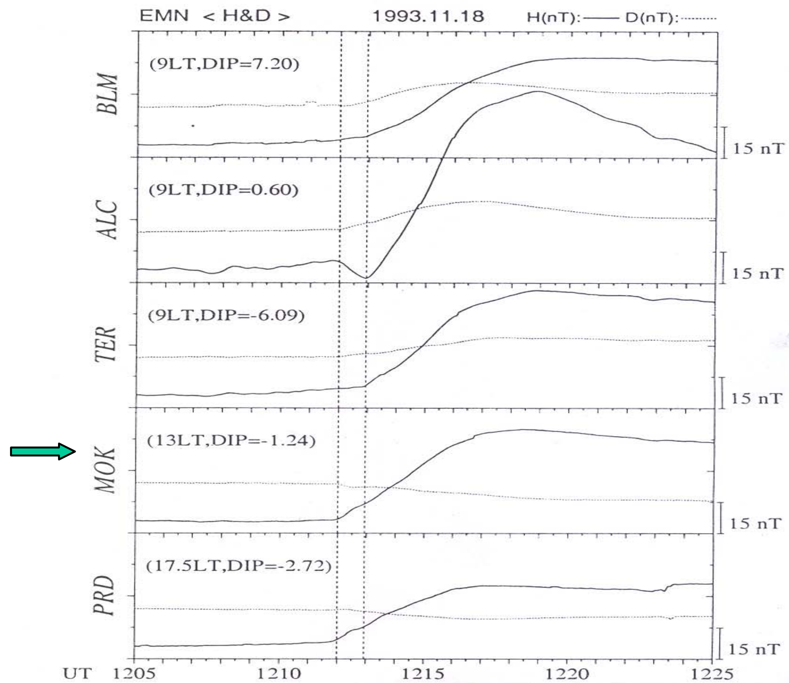

Sastri et al., JGR-A, Vol 106, 3905, 2001

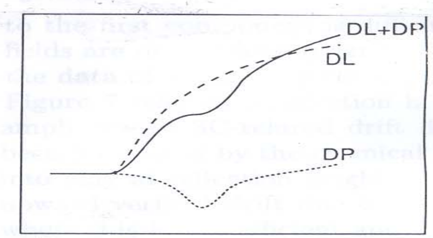

longitudinal (LT) profile of equatorial *pri* of *ssc**- presence (absence) of *pri* in forenoon sector (post-noon sector)-

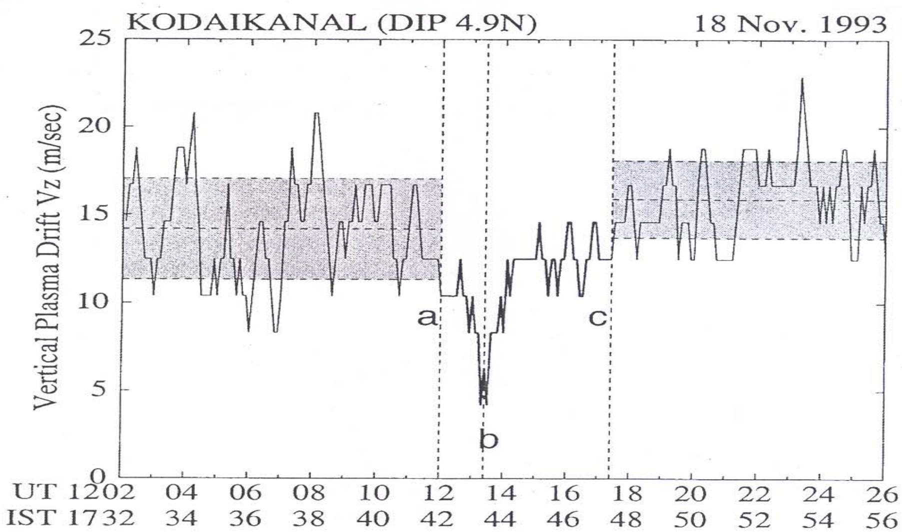

possible effect of morning side rotation of the twin-vortex ionospheric current system driven by FAC's - supported by theoretical calculations (orientation of causative IP shock)

gure 7. Time variation of F region vertical plasma drift V_z at Kodaikanal (dip 4.9°) in the lian zone. The vertical lines mark the different segments of the short-lived disturbance in V_z ociated with the SC. The average values of V_z and their standard deviations in the intervals or to and after the disturbance (shaded regions) are indicated by horizontal lines.

TAKEUCHI ET AL.: EFFECT OF SHOCK ORIENTATION ON SC

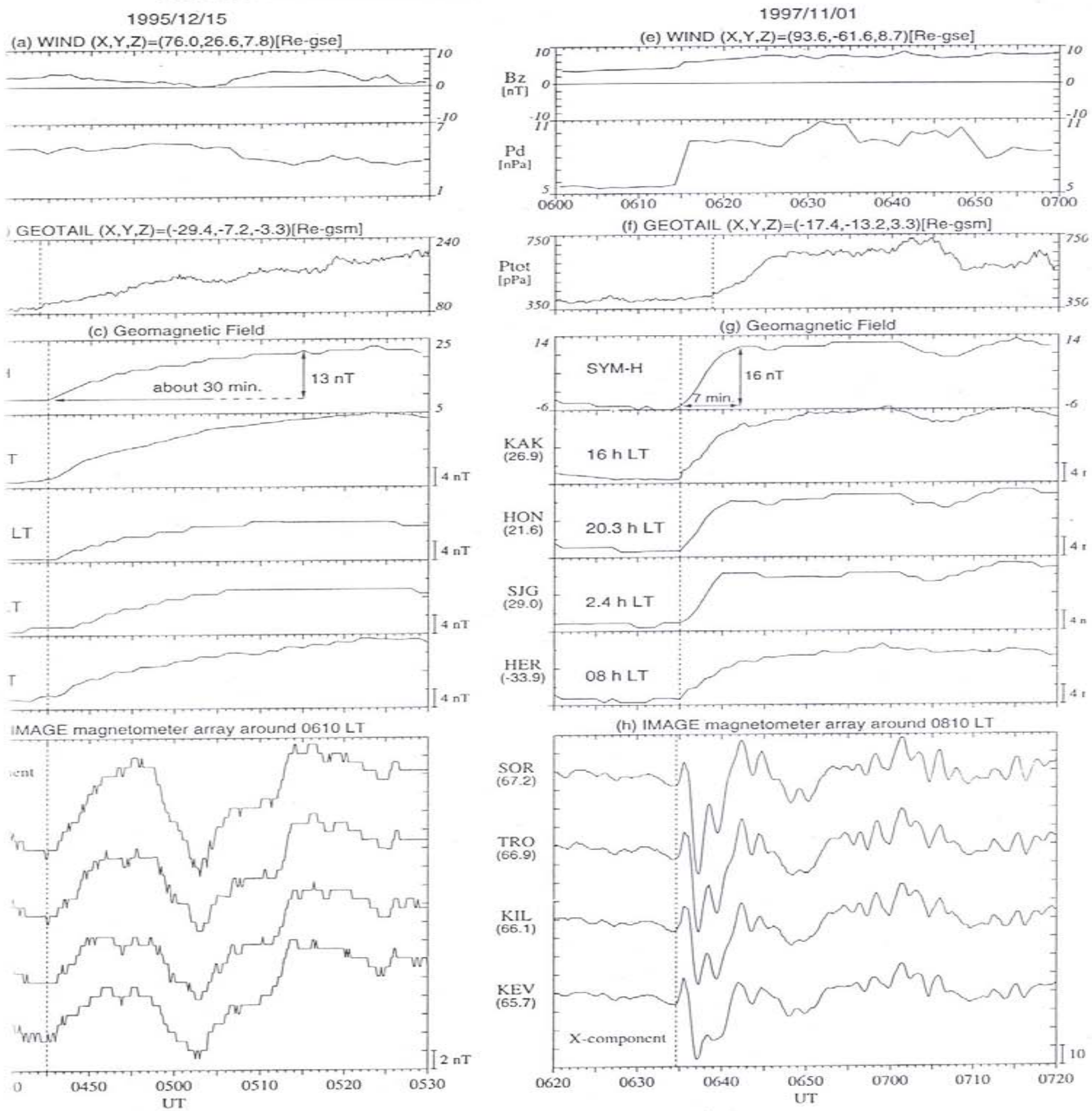

1. (a–d) An interplanetary shock and shock-related phenomena in the magnetosphere and on the
for 1 hour from 0430 to 0530 UT on 15 December 1995. (e–h) A typical SC event observed on 1
ber 1997. Observations in the solar wind from 0600 to 0700 UT and in the magnetosphere from
0720 UT are shown. The data set is the same as the left. Figures 1a and 1c show the north-south

Takeuchi et al., JGR-A, Vol 107, 1423, 2002.

ssc event of 15 Dec 1995- unusually large rise time of ~30 min (normal range 2-10 min)- due to oblique impact of IP shock

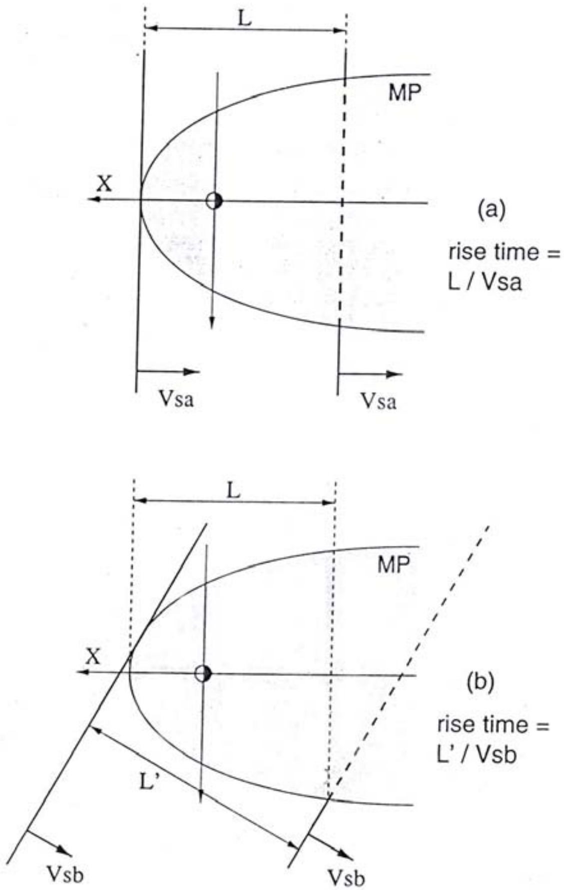

Figure 8. Model for the rise time of SC.

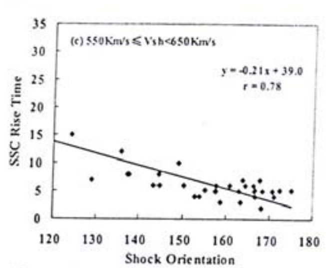

Figure 3. The SSC rise time as a function of shock orientation for IP shocks with speeds (a) 350–450 km/s, (b) 450–550 km/s, and (c) 550–650 km/s.

Case study

Takeuchi et al, JGR-A, 107, 1423, 2002

Statistical study of 225 IP shock-related *ssc* (events as seen in D_{st} index)

Wang et al – GRL, 33, L 14104, 2006

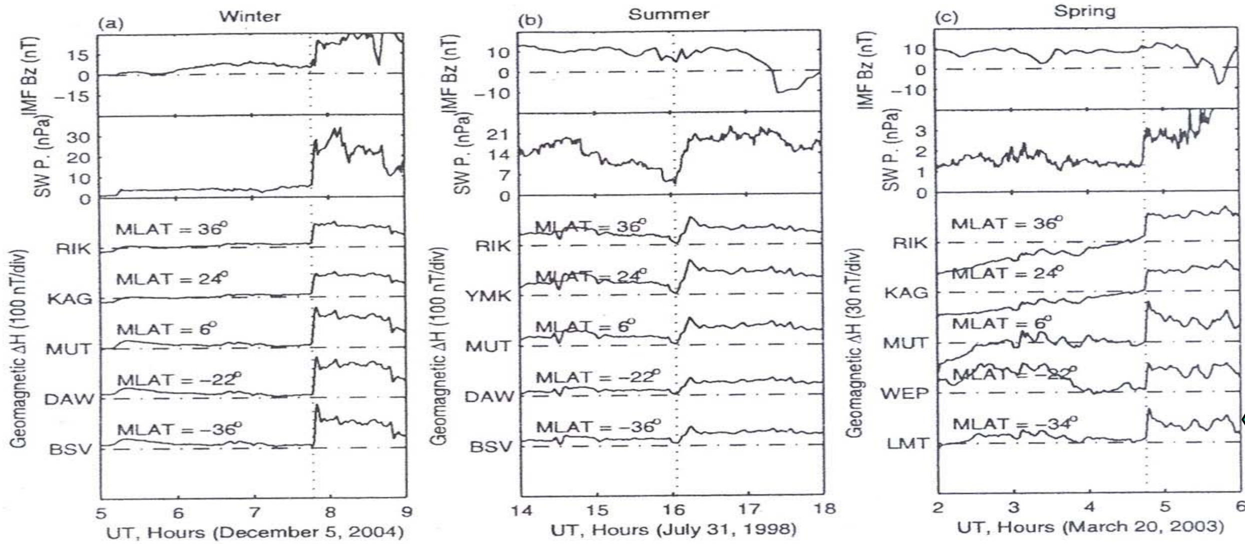

Figure 1. Sudden increases of the low-latitude geomagnetic field northward (*H*) component caused by solar wind pressure enhancements during northward interplanetary magnetic field (IMF). Figure 1a shows the IMF B_z, solar wind pressure, and geomagnetic *H* field in winter. Figures 1b and 1c show the cases in summer and spring, respectively. The magnetometer stations are Rikubetsu (RIK), Kagoshima (KAG), Yamakawa (YMK), Muntinlupa (MUT), Darwin (DAW), Birdsville (BSV), Weipa (WEP), and Learmonth (LMT). Magnetic latitude (MLAT) for each station is given in the figure.

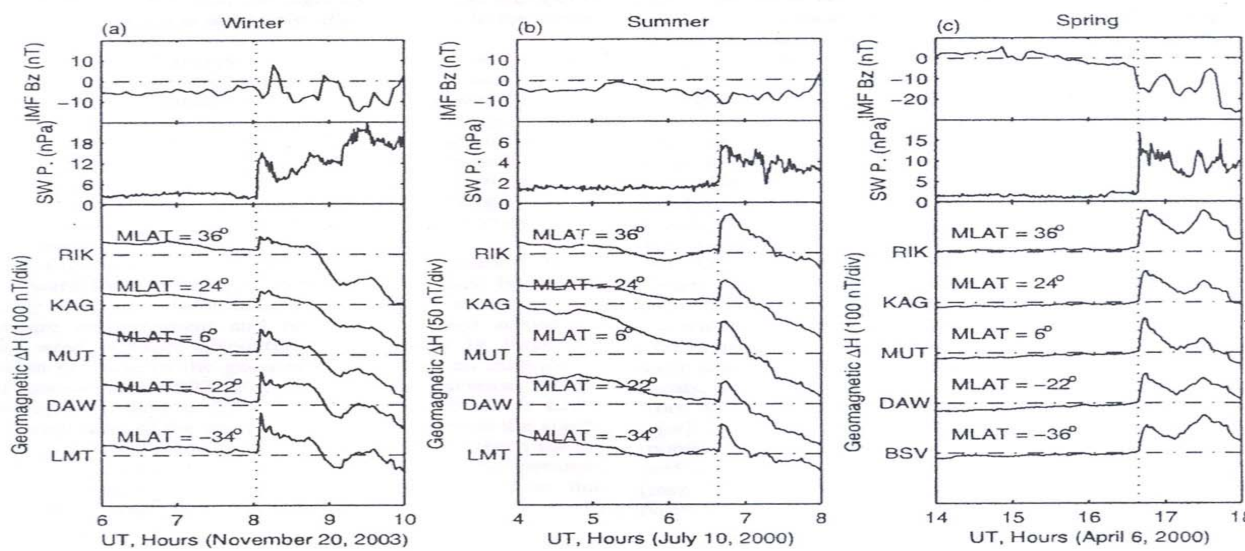

Figure 3. Sudden increases of the low-latitude geomagnetic field *H* component caused by solar wind pressure enhancements during southward IMF. Figure 3a shows the IMF B_z, solar wind pressure, and geomagnetic *H* field in winter. Figures 3b and 3c show the cases in summer and spring, respectively.

Huang and Yumoto, JGR-A, Vol. 111, A09316, 2006

Northward Bz

Season and Bz-dependent hemisphere asymmetry of *ssc* at low latitudes- tilt of Earth's magnetic axis (varies in the range 11-35°)

Southward Bz

(some) unsettled issues concerning equatorial manifestation of ssc's

1. Origin of the bi-modal response of equatorial dayside H-field (ssc and ssc*) to sudden magnetospheric compressions- external factors (IMF Bz, orientation of IP shock, magnitude enhancement of Pd [ΔP_d, $\Delta P_d/P_{d0}$) AND
   - propagation of *pri* to dayside dip equator (waveguide VS MHD waves)
2. Longitudinal pattern of *pri* chararacteristics (amplitude- absolute and relative to main impulse, *mi*); event-to-event variability and its origin; quantitative relationship of *pri* amplitude with the enhancement of P_d (ΔP_d, $\Delta P_d/P_{d0}$)
3. What factors control the dip equator enhancement of *mi* amplitude? what causes its event-to-event variability for a given station/local time? Why the dip equator enhancement not seen or the latitude profile of *mi* reversed in some *ssc* events in the afternoon sector, when counter-electrojet (CEJ) condition prevailed?

Further progress requires:

Studies

- with accurately characterized IP shocks [ambient IMF Bz, orientation of shock, magnitude & strength of the pressure enhancement (ΔP, $\Delta P/P_0$)],

- global data from suitably strengthened latitudinal and longitudinal (particularly for the dip equatorial region) networks of GPS-synchronized ground magnetometers with high -time resolution (1 s or better) AND

- space-borne magnetometers

+

- theoretical work (numerical simulations, innovative analytical formulations)

International collaborative / co-operative programs, IHY/ILWS/CAWSES can facilitate the progress


Thank You